



International Agreement Report

Mechanical Properties of Unirradiated and Irradiated Zr-1% Nb Cladding

Procedures and Results of Low Temperature Biaxial Burst Tests and Axial Tensile Tests

Prepared by

E. Kaplar, L. Yegorova, K. Lioutov, A. Konobeyev, N. Jouravkova
Nuclear Safety Institute of Russian Research Centre "Kurchatov Institute"
Kurchatov Square 1, Moscow 123182 Russian Federation

and

V. Smirnov, A. Goryachev, V. Prokhorov, O. Makarov, S. Yerebin, A. Svyatkin
State Research Centre "Research Institute of Atomic Reactors"
Dimitrovgrad 433510, Russian Federation

**Office of Nuclear Regulatory Research
U.S. Nuclear Regulatory Commission
Washington, DC 20555-0001**

April 2001

Prepared for

U.S. Nuclear Regulatory Commission, Institute for Protection and Nuclear Safety (France), and
Ministry of Science and Technologies (Russian Federation)

Published by

U.S. Nuclear Regulatory Commission

AVAILABILITY OF REFERENCE MATERIALS IN NRC PUBLICATIONS

NRC Reference Material

As of November 1999, you may electronically access NUREG-series publications and other NRC records at NRC's Public Electronic Reading Room at www.nrc.gov/NRC/ADAMS/index.html.

Publicly released records include, to name a few, NUREG-series publications; *Federal Register* notices; applicant, licensee, and vendor documents and correspondence; NRC correspondence and internal memoranda; bulletins and information notices; inspection and investigative reports; licensee event reports; and Commission papers and their attachments.

NRC publications in the NUREG series, NRC regulations, and *Title 10, Energy*, in the Code of *Federal Regulations* may also be purchased from one of these two sources.

1. The Superintendent of Documents
U.S. Government Printing Office
Mail Stop SSOP
Washington, DC 20402-0001
Internet: bookstore.gpo.gov
Telephone: 202-512-1800
Fax: 202-512-2250
2. The National Technical Information Service
Springfield, VA 22161-0002
www.ntis.gov
1-800-553-6847 or, locally, 703-605-6000

A single copy of each NRC draft report for comment is available free, to the extent of supply, upon written request as follows:

Address: Office of the Chief Information Officer,
Reproduction and Distribution
Services Section

U.S. Nuclear Regulatory Commission
Washington, DC 20555-0001

E-mail: DISTRIBUTION@nrc.gov

Facsimile: 301-415-2289

Some publications in the NUREG series that are posted at NRC's Web site address www.nrc.gov/NRC/NUREGS/indexnum.html are updated periodically and may differ from the last printed version. Although references to material found on a Web site bear the date the material was accessed, the material available on the date cited may subsequently be removed from the site.

Non-NRC Reference Material

Documents available from public and special technical libraries include all open literature items, such as books, journal articles, and transactions, *Federal Register* notices, Federal and State legislation, and congressional reports. Such documents as theses, dissertations, foreign reports and translations, and non-NRC conference proceedings may be purchased from their sponsoring organization.

Copies of industry codes and standards used in a substantive manner in the NRC regulatory process are maintained at—

The NRC Technical Library
Two White Flint North
11545 Rockville Pike
Rockville, MD 20852-2738

These standards are available in the library for reference use by the public. Codes and standards are usually copyrighted and may be purchased from the originating organization or, if they are American National Standards, from—

American National Standards Institute
11 West 42nd Street
New York, NY 10036-8002
www.ansi.org
212-642-4900

Legally binding regulatory requirements are stated only in laws; NRC regulations; licenses, including technical specifications; or orders, not in NUREG-series publications. The views expressed in contractor-prepared publications in this series are not necessarily those of the NRC.

The NUREG series comprises (1) technical and administrative reports and books prepared by the staff (NUREG-XXXX) or agency contractors (NUREG/CR-XXXX), (2) proceedings of conferences (NUREG/CP-XXXX), (3) reports resulting from international agreements (NUREG/IA-XXXX), (4) brochures (NUREG/BR-XXXX), and (5) compilations of legal decisions and orders of the Commission and Atomic and Safety Licensing Boards and of Directors' decisions under Section 2.206 of NRC's regulations (NUREG-0750).

DISCLAIMER: This report was prepared under an international cooperative agreement for the exchange of technical information. Neither the U.S. Government nor any agency thereof, nor any employee, makes any warranty, expressed or implied, or assumes any legal liability or responsibility for any third party's use, or the results of such use, of any information, apparatus, product or process disclosed in this publication, or represents that its use by such third party would not infringe privately owned rights.

NUREG/IA-0199
IPSN 01-16
NSI RRC 2241



International Agreement Report

Mechanical Properties of Unirradiated and Irradiated Zr-1% Nb Cladding

Procedures and Results of Low Temperature Biaxial Burst Tests and Axial Tensile Tests

Prepared by
E. Kaplar, L. Yegorova, K. Lioutov, A. Konobeyev, N. Jouravkova
Nuclear Safety Institute of Russian Research Centre "Kurchatov Institute"
Kurchatov Square 1, Moscow 123182 Russian Federation

and

V. Smirnov, A. Goryachev, V. Prokhorov, O. Makarov, S. Yeremin, A. Svyatkin
State Research Centre "Research Institute of Atomic Reactors"
Dimitrovgrad 433510, Russian Federation

**Office of Nuclear Regulatory Research
U.S. Nuclear Regulatory Commission
Washington, DC 20555-0001**

April 2001

Prepared for
U.S. Nuclear Regulatory Commission, Institute for Protection and Nuclear Safety (France), and
Ministry of Science and Technologies (Russian Federation)

**Published by
U.S. Nuclear Regulatory Commission**

ABSTRACT

This report contains the description of the test conditions, procedures, and main results of the following types of mechanical tests of unirradiated and irradiated Zr-1%Nb cladding:

- biaxial burst tests with liquid pressurized tube specimens in the temperature range 293–723 K;
- uniaxial tensile tests in axial direction with tube specimens in the temperature range 293–1200 K.

Results of these tests are compared with test results obtained in 1997–1999 using simple ring specimens (293–1200 K) and gas pressurized tube specimens (900–1400 K).

TABLE OF CONTENTS

	Page
1. EXECUTIVE SUMMARY	1.1
1.1. Introduction	1.1
1.2. Program of tests.....	1.1
1.3. Selection of test parameters and ranges	1.4
2. CONDITIONS, PROCEDURES AND RESULTS OF BIAXIAL BURST TESTS	2.1
2.1. Test facility for biaxial burst tests.....	2.1
2.2. Test procedures and measured parameters.....	2.4
2.3. Results of biaxial burst tests.....	2.7
3. CONDITION, PROCEDURES AND RESULTS OF AXIAL TENSILE TESTS.....	3.1
3.1. Test procedure and specimen design.....	3.1
3.2. Results of axial tensile tests	3.5
4. CONCLUSIONS	4.1

LIST OF FIGURES

	Page
Fig. 1.1. Structure of the program to obtain generalized data base.....	1.2
Fig. 2.1. Burst test facility.....	2.1
Fig. 2.2. Post-test appearance of specimens pressurized by gas and liquid.	2.2
Fig. 2.3. Sealing devices.....	2.3
Fig. 2.4. Specimen temperatures versus specimen length and test temperature.	2.4
Fig. 2.5. Typical time history of burst test.	2.5
Fig. 2.6. Method to determine the axial radius of burst region curvature.....	2.6
Fig. 2.7. Burst pressure versus temperature.	2.10
Fig. 2.8. Circumferential elongation versus temperature.....	2.11
Fig. 2.9. True hoop stress at rupture versus temperature.	2.11
Fig. 3.1. Design of tube specimen according to the U.S. Standard.....	3.1
Fig. 3.2. Design of tube specimen according to the French Standard.....	3.1
Fig. 3.3. Design of tube specimen according to the Russian Standard.	3.2
Fig. 3.4. Design of Zr-1%Nb tube specimen used for axial tensile tests.	3.3
Fig. 3.5. Load-displacement curve.	3.4
Fig. 3.6. Increment of interval between marks versus specimen length.	3.4
Fig. 3.7. Ultimate strength versus temperature.	3.6
Fig. 3.8. Yield stress versus temperature.	3.7
Fig. 3.9. Total elongation versus temperature.....	3.8
Fig. 3.10. Uniform elongation versus temperature ($\dot{\epsilon}=2 \cdot 10^{-3} \text{ s}^{-1}$)	3.8
Fig. 3.11. US/YE ratio versus temperature.	3.9

LIST OF TABLES

	Page
Table 1.1. Matrix of burst tests.	1.2
Table 1.2. Matrix of axial tensile tests.	1.3
Table 1.3. Parameters of unirradiated specimens.	1.3
Table 1.4. Parameters of irradiated specimens.	1.3
Table 2.1. Sensitivity of specimen temperature at the burst to the type of working medium.....	2.3
Table 2.2. Set of procedures to determine specimen geometric parameters after burst tests.	2.6
Table 2.3. Appearance of unirradiated cladding specimens versus biaxiality and temperature.	2.7
Table 2.4. Appearance of irradiated cladding specimens versus biaxiality and temperature.	2.8
Table 2.5. Appearance of cross-sections of unirradiated and irradiated cladding specimens in the burst region versus biaxiality and temperature.	2.8
Table 2.6. Major results of burst tests.....	2.9
Table 2.7. Correlations for burst parameters versus temperature, biaxiality and type of cladding.	2.11
Table 3.1. Appearance of unirradiated specimens after tensile tests.	3.5
Table 3.2. Main results of axial tensile tests.	3.5
Table 3.3. Results of simple ring tensile tests on irradiated Zr-1%Nb cladding (strain rate 0.002 1/s).....	3.7

1. EXECUTIVE SUMMARY

1.1. Introduction

There is significant research today on the confirmation of fuel element safety in commercial light-water reactors under accident conditions up to high fuel burnup (50–70 MWd/kg U). The development of a database on mechanical characteristics of highly irradiated fuel claddings is one of the relevant components of this work. With the mechanical characteristics determining the behavior of cladding during a reactivity-initiated accident (RIA) and during the initial stage of the loss-of-coolant accident (LOCA), research to develop a database of mechanical characteristics of Zr-1%Nb claddings was therefore initiated in 1997. This research was conducted with financial support of Ministry of Science and Technologies of the Russian Federation, AO Mashinostroitelny zavod (Russia, Elektrostal), U.S. Nuclear Regulatory Commission (U.S.), and Institute for Protection and Nuclear Safety (France). The work consists of four basic stages:

1. uniaxial tensile tests in transverse direction with simple ring specimens at temperature range 293–1200 K;
2. biaxial burst tests with gas pressurized tube specimens at temperature range 900–1400 K;
3. biaxial burst tests with liquid pressurized tube specimens at temperature range 293–723 K;
4. uniaxial tensile tests in axial direction with tube specimens at temperature range 293–1200 K.

The first two stages were completed in 1998. The outcomes of these tests were used to make correlations of the basic mechanical characteristics of the unirradiated and irradiated Zr-1%Nb alloy claddings versus temperature and strain rate. These correlations were introduced in thermal mechanical codes FRAT-T6 and SCANAIR. The upgraded versions of both codes were verified by the results of re-fabricated fuel elements test in the IGR reactor under RIA conditions. The detailed description of these researches and their outcomes are presented in [1, 2, 3].

Later stages of this research were held in 1999 and 2000. Tasks, techniques and outcomes of these tests are described in the present report.

1.2. Program of tests

The recent stages of mechanical tests of unirradiated and irradiated Zr-1%Nb claddings were held to accomplish the following basic tasks:

- a. to update the previously obtained data base by outcomes of axial tensile tests and biaxial burst tests (with different biaxiality ratio);
- b. to conduct the cross-verification of all types of tests results;
- c. to estimate the anisotropy effects for unirradiated and irradiated Zr-1%Nb claddings.

In accordance with these tasks were determined the following technical requirements to each test stage (see Fig. 1.1):

- biaxial burst tests:
 - ⇒ temperature range 293–723 K;
 - ⇒ biaxiality ratio 1 and 2;
 - ⇒ pressure increase rate 1 MPa/s;
- axial tensile tests:

⇒ temperature range 293–1200 K;

⇒ strain rate $2 \cdot 10^{-3}$ 1/s.

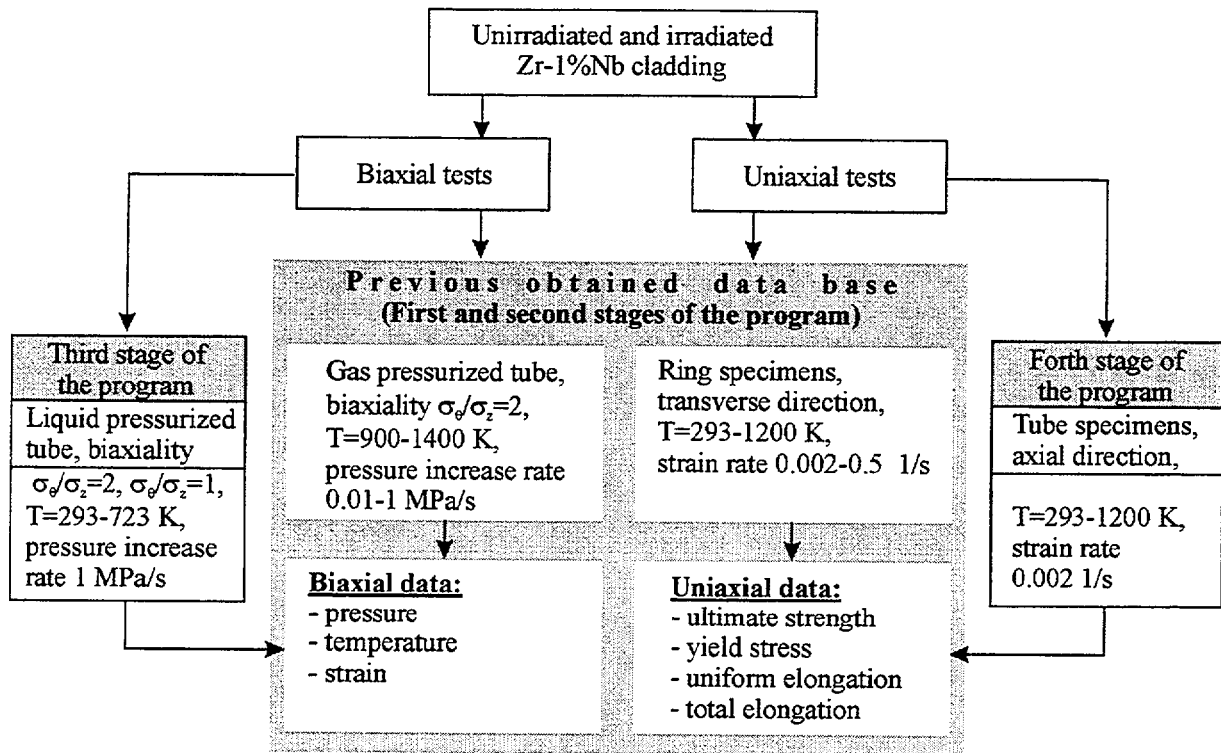


Fig. 1.1. Structure of the program to obtain generalized data base.

These requirements were used as the basis to explore burst and axial test matrixes presented in Table 1.1, Table 1.2.

Table 1.1. Matrix of burst tests.

Temperature (K)	Number of tests			
	Unirradiated		Irradiated	
	Biaxiality 2	Biaxiality 1	Biaxiality 2	Biaxiality 1
293	2	—	—	—
323	1	1	—	—
423	1	1	1	2
543	2	2	1	2
623	1	1	—	—
723	4	2	2	2
Σ	11	7	4	6

Table 1.2. Matrix of axial tensile tests.

Temperature (K)	Number of tests	
	Unirradiated	Irradiated
293	1	–
323	–	1
423	1	2
543	1	2
723	2	2
1000	1	1
1200	1	–
Σ	7	8

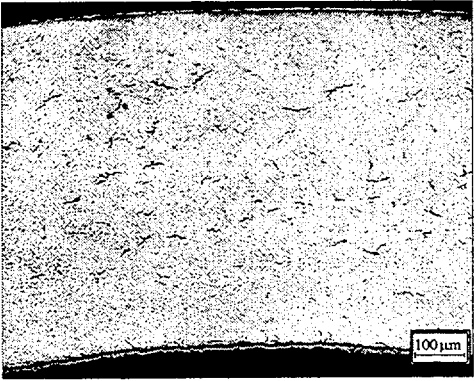
It should be noted that cladding specimens for mechanical tests of both types were made of a material similar to that of the cladding specimens used in the first two stages of the program. So, by analogy with the previously performed tests, standard fully recrystallized VVER-1000 commercial tubes were used for unirradiated specimens (see Table 1.3).

Table 1.3. Parameters of unirradiated specimens.

Chemical composition of Zr-1%Nb cladding (% by weight)		Specimens characteristics	
• Nb	0.9–1.1	• outer diameter	9.11 mm
• Fe	0.05	• inner diameter	7.72 mm
• Cr	0.02	• outer ZrO ₂ thickness (less than)	1 μ m
• Ni	0.05	• length:	
• Fe+Cr+Ni	0.12	⇒ burst tests	150 mm
• O ₂	0.11	⇒ axial tests	50 mm

The same approach has been applied for irradiated specimens manufactured from two commercial VVER-1000 fuel elements (#165, 154) irradiated in Unit 5 of NovoVoronozh Nuclear Power Plant during four years as a part of fuel assembly #4108. Average burnup of fuel elements sections used for manufacturing of specimens was about 48 MWd/kg U. The main parameters of irradiated cladding are presented in Table 1.4.

Table 1.4. Parameters of irradiated specimens.

Specimens characteristics		Cladding microstructure
• outer diameter	9.068–9.096 mm	
• cladding thickness	0.54–0.84 mm	
• outer ZrO ₂ thickness	3–5 μ m	
• inner ZrO ₂ thickness (less than)	1 μ m	
• hydrogen concentration (ppm)	51–57	
• hydride orientation coefficient	0.42	
• length:		
⇒ burst tests	150 mm	
⇒ axial tests	50 mm	

1.3. Selection of test parameters and ranges

The selection of test parameters and ranges was substantially determined by the fact that these tests were conducted with the purpose of updating and improvement of the previously obtained database. The inter-coupling of all test types for development of a generalized database is illustrated on Fig. 1.1.

Tests with different stress biaxiality ratio.

- in the high-temperature zone the material is practically isotropic;
- in the high-temperature zone the loading of a cladding is determined by the gas pressure, the biaxiality ratio at such loading equals 2;
- there are no data on burst tests in low-temperature zone;
- the low-temperature zone is of interest from the point of view of the pellet cladding mechanical interaction at which the biaxiality ratio can vary from 2 to 1, depending on the contact condition;
- the pellet cladding mechanical interaction is characterized by high values of the cladding strain rate.

Axial direction tests.

The temperature range of axial direction tests has been set the same as for ring tensile tests, because the power law parameters are determined just by results of uniaxial tests. The tests were conducted only for a basic strain rate, because the strain rate sensitivity exponent describing the influencing of the velocity has been determined earlier with a significant amount of experimental data.

2. CONDITIONS, PROCEDURES AND RESULTS OF BIAXIAL BURST TESTS

2.1. Test facility for biaxial burst tests

A special test facility was designed for conducting biaxial tube burst tests in compliance with the following requirements:

- Temperature range 20–450°C;
- Working pressure range 40–200 MPa;
- Pressure increase rate – up to 2 MPa/s;
- Axial load up to 10 kN;
- Tangential and axial stress synchronization at a pre-selected ratio;
- Non-uniformity of the specimen temperature not exceeding of $\pm 10^\circ\text{C}$.

Schematic Diagram of the test facility, developed to meet these requirements, is shown in Fig. 2.1.

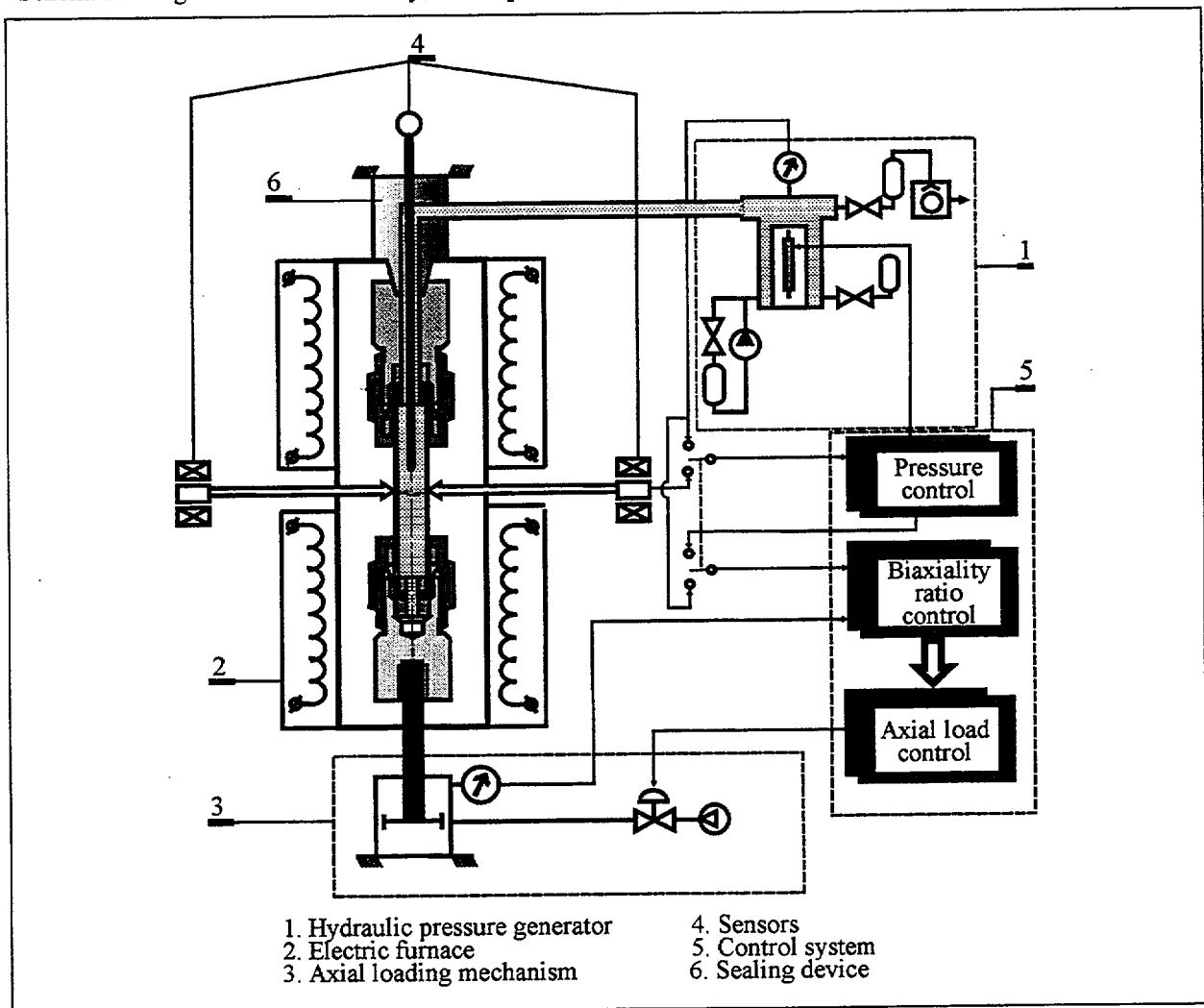


Fig. 2.1. Burst test facility.

The specimen was placed inside the electric furnace to ensure the required specimen temperature. Pressure in the specimen was created with the use of a hydraulic pressure generator. A special mechanism was used to provide additional axial stress, which varied in synchronism with the pressure inside the specimen at a

pre-selected ratio between tangential and axial stresses (1 or 2). With the axial loading mechanism switched off, gas pressure in the specimen provided a biaxiality ratio of 2. With the axial loading mechanism switched on, the biaxiality ratio was maintained at 1 with the use of the control system including axial loading control and biaxiality ratio control. Special sealing device prevented any leakage from the specimen during the test.

A series of special research was conducted during development of the test facility to resolve the following problems:

- selection of working medium inside test specimens;
- development of sealing devices for specimens;
- ensuring stability of selected temperature.

Selection of working medium.

Analysis showed that results of specimen gas pressurization would be difficult to interpret. This is caused by the fact that high kinetic energy of gas, flowing from the specimen at burst, produces additional bending and tearing of the ruptured area. Therefore, decision was taken to give up gas medium and use liquid pressurization instead, because, the liquid medium pressure drops practically instantaneously and causes no additional damage (see Fig. 2.2). However, liquids are not normally used as working medium in the installations of this kind, since it is very difficult to find a liquid, which is free from phase transformations, and will not inflame or chemically react with the specimen material throughout the entire temperature range. To solve this problem we had to conduct special analytical research, which allowed us to recommend several types of liquids for this installation. Analysis of the results of preliminary tests performed on these liquids made it possible to select silicone oil "Sopolymer-3" as the working medium. Boiling point, ignition temperature and flash point of this oil exceed 450°C.

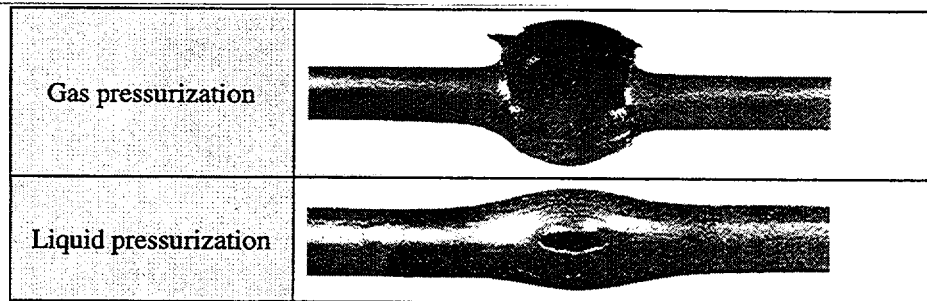


Fig. 2.2. Post-test appearance of specimens pressurized by gas and liquid.

Sealing problem of specimen.

Development of a sealing device for specimens also was a challenging task. The main challenge was to seal the specimen having high internal pressure at axial loads. Welding of irradiated specimens was unacceptable, because it could lead to annealing of irradiation damage, which could change mechanical properties of these specimens. As a result of the design and process analyses, and a series of scoping tests, three types of sealing devices were developed for three types of specimens used (unirradiated specimen, irradiated specimen without axial loading, irradiated specimen with axial loading). For the design of these sealing devices, see Fig. 2.3. All three designs use one sealing principle - sealing with a copper gasket placed between the cone and the nut. The difference is mainly in the number of parts used to increase the required axial load.

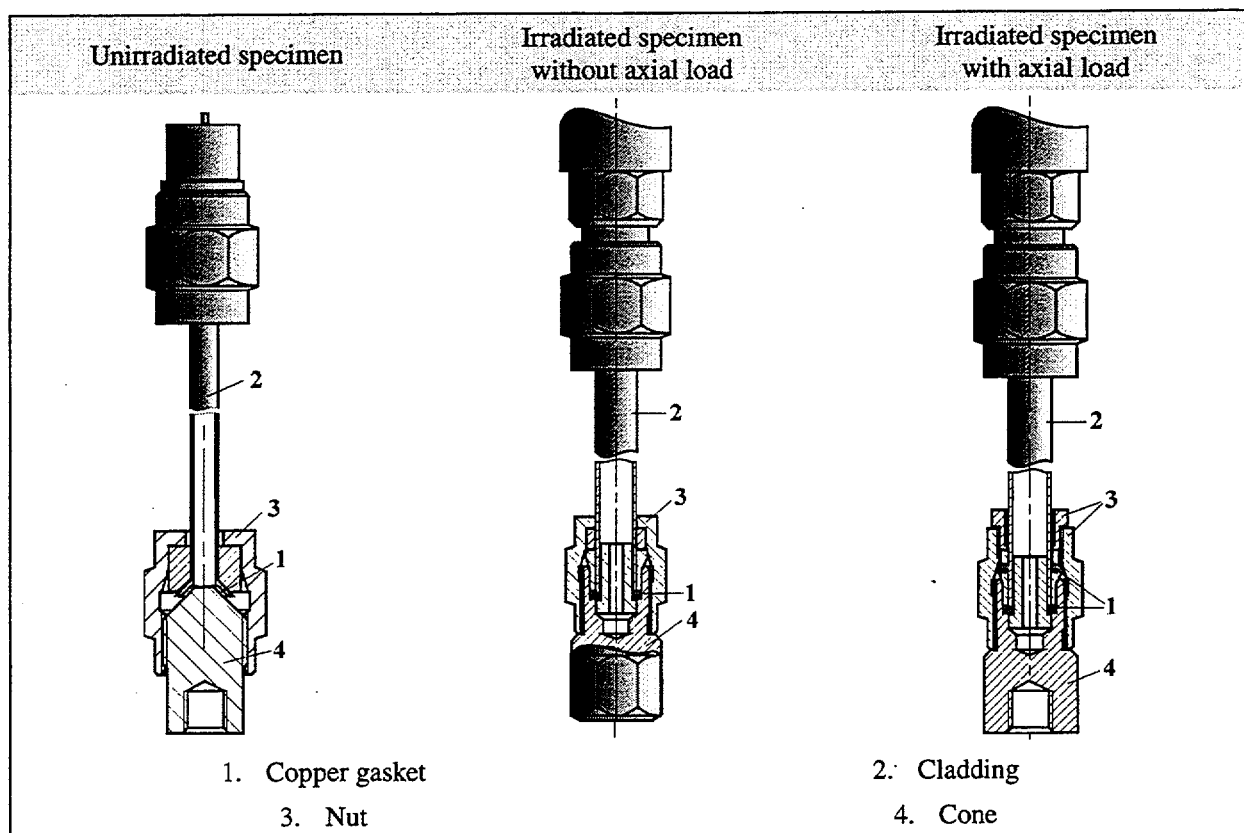


Fig. 2.3. Sealing devices.

Stability of specimen temperature.

Analysis of the first version of the burst test facility showed that deformation of a pressurized specimen resulted in the increase of its volume, which, in its turn, increased the inflow of working medium from the supply pipeline, where the working medium was at an ambient temperature. As a result, the working medium and the specimen temperature dropped. The quantitative effect is different for gas and liquid. Results of calculations, presented in Table 2.1, demonstrate that replacement of gas with liquid causes a more significant temperature drop in the specimen. This happens due to higher specific heat and density of liquids.

Table 2.1. Sensitivity of specimen temperature at the burst to the type of working medium.

Test parameters	Working medium	
	Liquid	Gas
Test temperature (°C)	270	270
Burst pressure (MPa)	60	60
Drop of working medium temperature (°C)	-53	-53
Drop of specimen temperature (°C)	-35	-9

To prevent this effect from influencing the test results the facility design was modified to introduce a heater for the supply pipeline. The next step in this research was aimed at checking uniformity of specimen temperature versus length. Results of special temperature measurements performed in steps of 10 mm at different nominal temperature levels are shown in Fig. 2.4. The obtained results indicate that temperature non-uniformity over the specimen length for all the tested condition does not exceed $\pm 5^\circ\text{C}$.

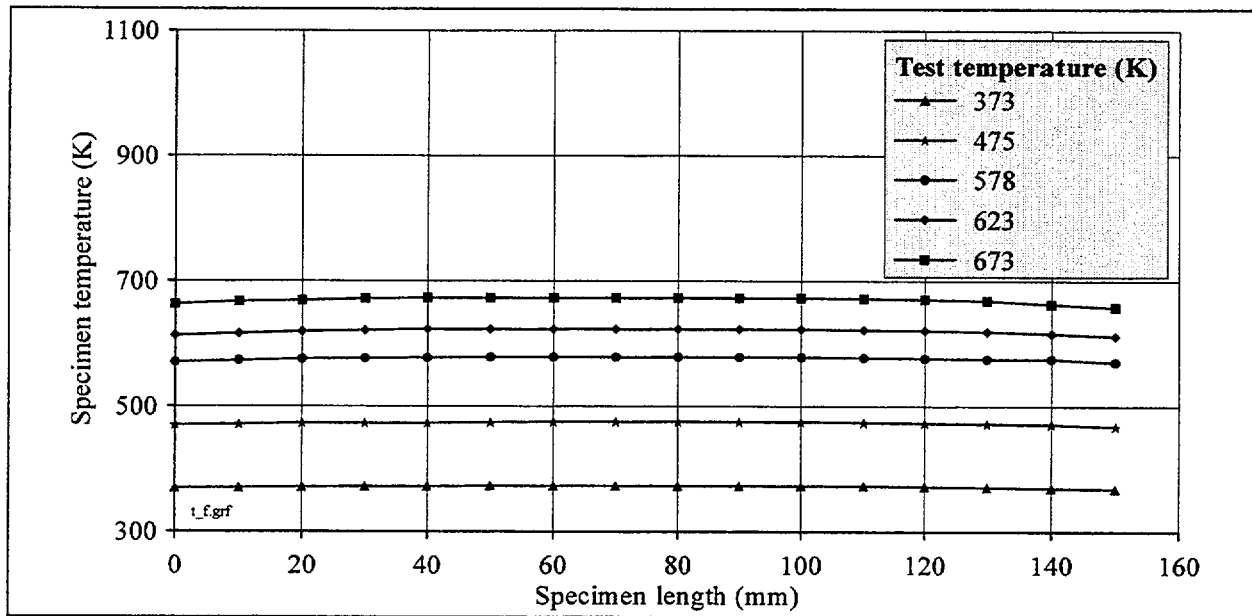


Fig. 2.4. Specimen temperatures versus specimen length and test temperature.

2.2. Test procedures and measured parameters

The burst test procedure included three steps:

1. preparation;
2. testing;
3. post-test examinations.

Test preparation procedure was as follows:

- sealing devices were attached to the specimen;
- vertically installed specimen was filled with liquid and sealed;
- specimen pressurization was performed to test it for leakage;
- the specimen was installed in the electric furnace heated to the specified test temperature;
- axial loading mechanism was attached to the lower end of the specimen for the axial loading test;
- specimen temperature stabilization was provided by holding it in the furnace for the specified time period.

The main step of the test was initiated upon actuation of the hydraulic pressure generator (see Fig. 2.5). Hydraulic pressure generator operated to increase pressure in the specimen to be in compliance with the test scenario. The average pressure increase rate was 1 MPa/s. The following parameters were measured during this test versus time:

- temperature in electric furnace;
- temperature of specimen;
- pressure inside specimen;
- axial load;
- increment of specimen outer diameter.

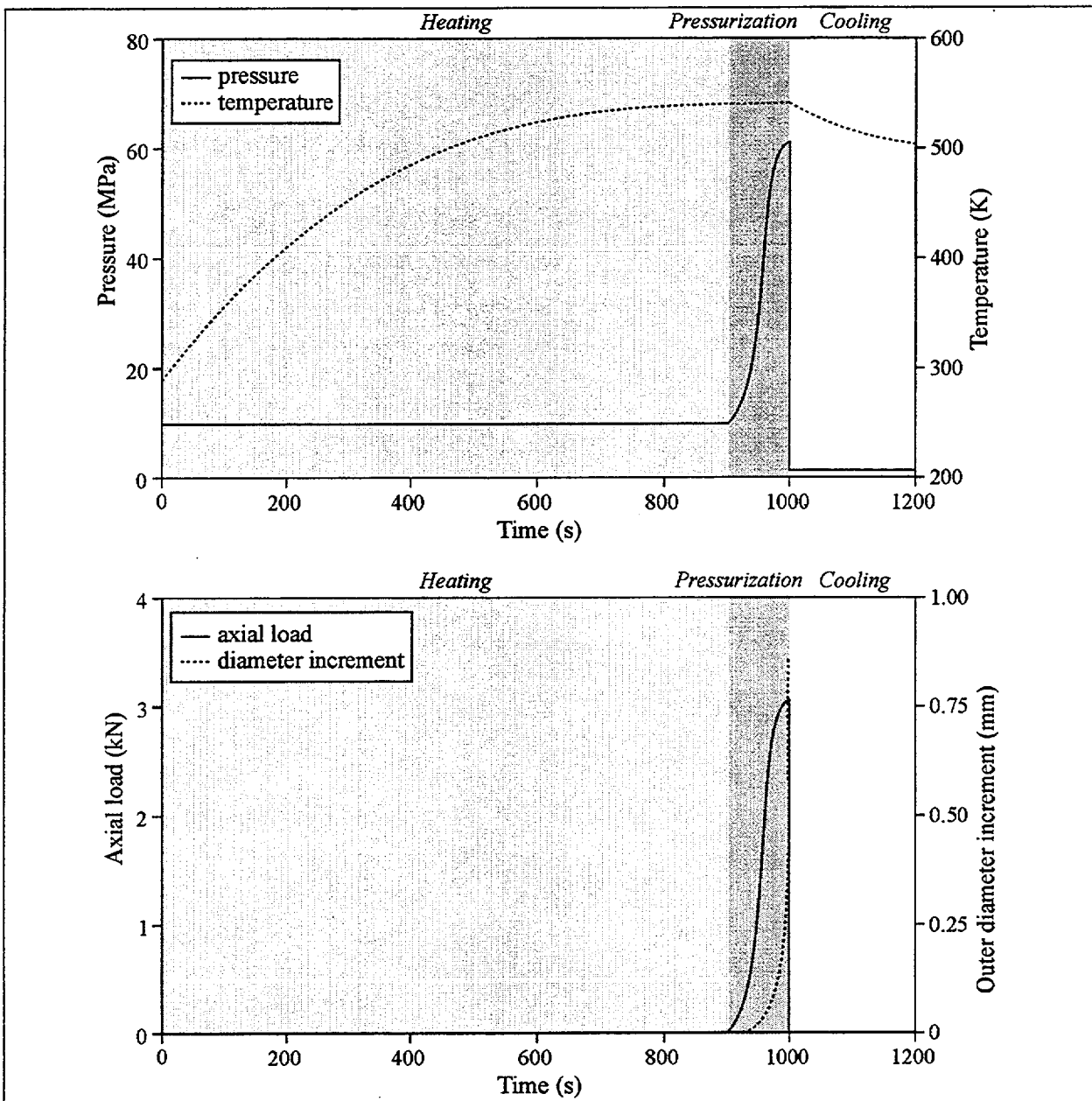


Fig. 2.5. Typical time history of burst test.

During the test, the temperature in electric furnace was maintained with an accuracy of $\pm 5^{\circ}\text{C}$. Specimen temperature measurement accuracy was also $\pm 5^{\circ}\text{C}$. Liquid pressure measurement accuracy was ± 1 MPa up to 100 MPa, and ± 5 MPa above 100 MPa. Axial load measurement accuracy was ± 0.2 kN.

After the biaxial tube burst tests were completed all specimens were subjected to post-tests examinations, including the following procedures:

- photography;
- profilometry;
- preparation and photographing of metallographic cross-section of the burst region;
- computer processing of the whole set of photographs for:
 - \Rightarrow determination of the middle line profile;
 - \Rightarrow measurement of the cladding thickness;

- ⇒ measurement of the axial radius of the burst region curvature;
- ⇒ measurement of the circumferential elongation;
- ⇒ measurement of the circumferential radius of the burst region curvature.

Previously developed methodological approaches to this research are described in [1]. Brief characteristics of the procedures used for the data determination are described in Table 2.2 and Fig. 2.6.

Table 2.2. Set of procedures to determine specimen geometric parameters after burst tests.

Specimen parameter	Basis of procedure
1. Outer diameter of cladding	Profilometry of specimen in four azimuth directions
2. Middle line profile	Splitting of computer image of the cladding cross-section into sections at adequately small azimuth intervals, finding the points corresponding to half cladding thickness in the center of each section and plotting the envelope through all the obtained points.
3. Cladding thickness	Measuring of cladding thickness in the middle of previously determined azimuth intervals, subsequent integration of the obtained data file to determine average value of the cladding thickness.
4. Axial radius of the burst region curvature (r_z)	See Fig. 2.6.
5. Circumferential elongation of specimen (ε_θ)	Finding absolute difference between the length of the middle line before and after the test with normalization for the middle line length before test (in percent).
6. Circumferential radius of the burst region curvature (r_θ)	$r_\theta = r_{\theta_0} \left(1 + \frac{\varepsilon_\theta}{100}\right),$ <p>where r_{θ_0} = radius of middle line of cladding (as fabricated)</p> <p>ε_θ = circumferential elongation.</p>

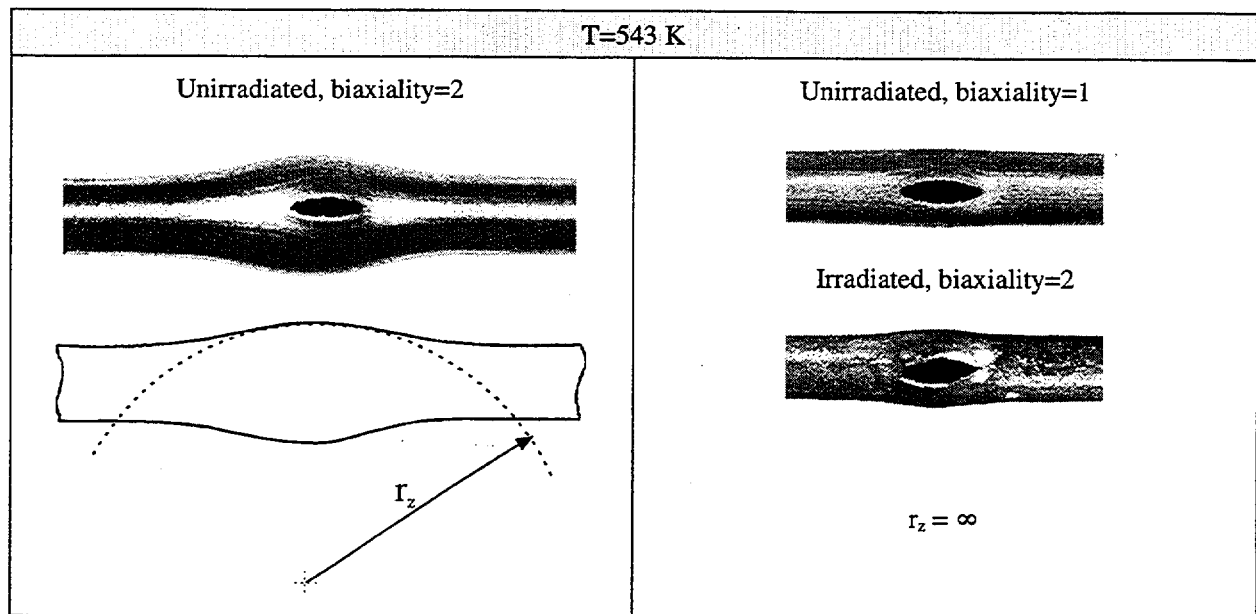


Fig. 2.6. Method to determine the axial radius of burst region curvature.

2.3. Results of biaxial burst tests

In accordance with research plan, 28 burst tests were conducted. Qualitative test results are contained in Table 2.3–Table 2.5.

Table 2.3. Appearance of unirradiated cladding specimens versus biaxiality and temperature.

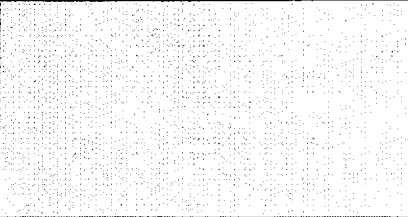
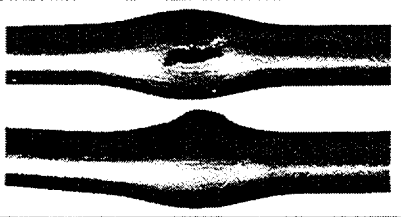
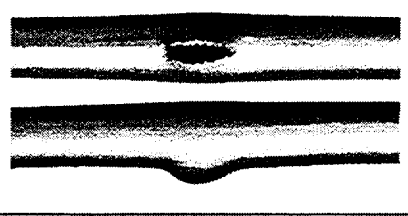
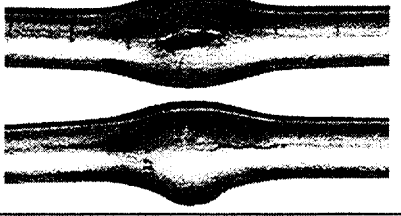
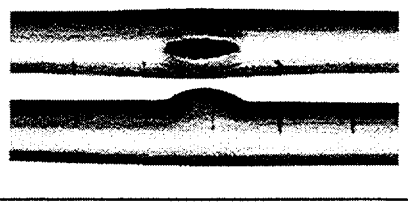



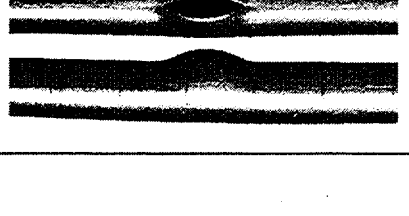

Temperature (Number of test)	Biaxiality=1	Biaxiality=2
293 K (HBO-3)		
323 K (E50L, E50)		
423 K (E150L, E150)		
543 K (H270-5L, H270-4)		
723 K (E450L, H50-6)		

Table 2.4. Appearance of irradiated cladding specimens versus biaxiality and temperature.

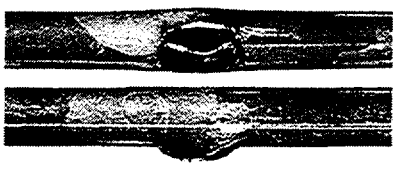

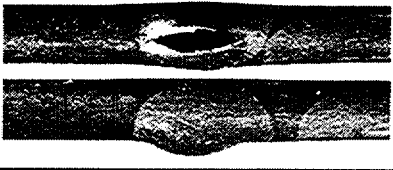
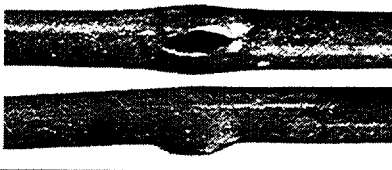
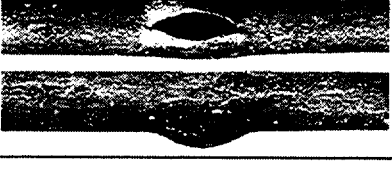
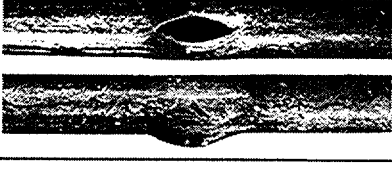
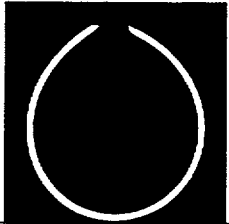
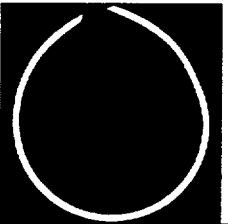
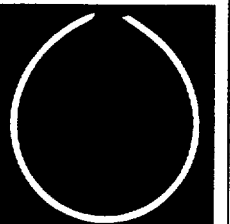
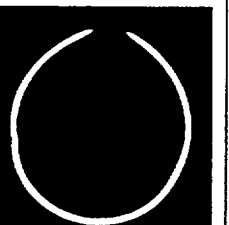
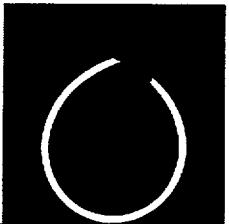
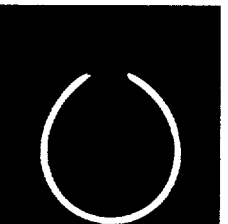

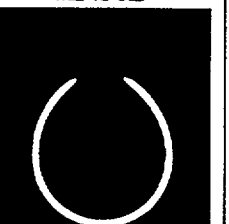
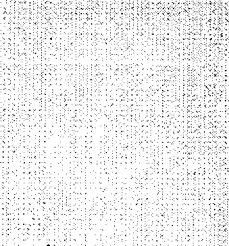

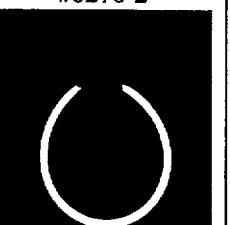
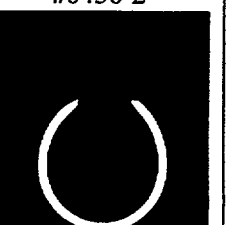

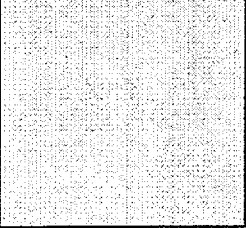
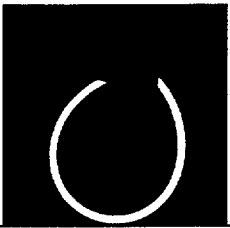

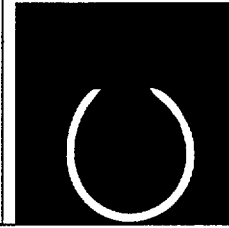
Temperature (Number of test)	Biaxiality=1	Biaxiality=2
423 K (0150-2L, 0150-2)		
543 K (0270-1L, 0270-2)		
723 K (0450-2L, 0450-2)		

Table 2.5. Appearance of cross-sections of unirradiated and irradiated cladding specimens in the burst region versus biaxiality and temperature.

Type of cladding and type of biaxiality	Temperature and test number			
	293–323 K	423 K	543 K	723 K
Unirradiated cladding (biaxiality=2)	#H20-1 	#E150 	#270-4 	#H450-6 
	#E50L 	#E150L 	#H270-5L 	#E450L 
Irradiated cladding (biaxiality=2)		#0150-2 	#0270-2 	#0450-2 
				

Type of cladding and type of biaxiality	Temperature and test number			
	293–323 K	423 K	543 K	723 K
Irradiated cladding (biaxiality=1)		#0150-2L 	#0270-1L 	#0450-2L 

Analysis of these results allows us to draw the following conclusions regarding the trends in the cladding mechanical behavior under these conditions:

- circumferential elongation reduces with the increase of temperature;
- biaxiality ratio drop from 2 to 1 causes significant reduction of circumferential elongation of unirradiated cladding, while irradiated cladding remains less sensitive to this parameter.

Quantitative assessment of the test results was performed on the basis of the source data given in Table 2.6.

Table 2.6. Major results of burst tests.

Test No.	Temperature (K)	Burst pressure (MPa)	Axial load at burst (N)	Circumferential elongation (%)	Wall thickness (mm)	Axial radius of curvature (r_z) (mm)	Circumferential radius of curvature (r_θ) (mm)
<i>Unirradiated</i>							
H20-1	293	88	–	60	0.54	30	6.75
H20-3	293	94	–	67	0.57	30	7.03
E50	323	85	–	79	0.54	30	7.54
E50L	323	94	4630	25	0.58	∞	5.30
E150	423	68	–	77	0.56	Not measured	Not measured
E150L	423	76	3750	21	0.57	Not measured	Not measured
H270-3	543	52	–	74	0.54	34.7	7.34
H270-4	543	54	–	75	0.55	36.7	7.38
H270-5L	543	60	3240	19	0.56	∞	5.01
H270-6L	543	61	2910	16	0.59	∞	4.90
E350	623	45	–	Not measured	Not measured	Not measured	Not measured
E350L	623	48	2380	Not measured	Not measured	Not measured	Not measured
E450	723	40	–	56	0.59	Not measured	Not measured
E450L	723	41	2000	18	0.52	Not measured	Not measured
H450-2	723	43	–	62	0.52	30	6.86
H450-5	723	42	–	69	0.55	30	7.15
H450-6	723	40	–	61	0.54	30	6.78
H450-7L	723	44	2190	16	0.58	∞	4.92

Test No.	Temperature (K)	Burst pressure (MPa)	Axial load at burst (N)	Circumferential elongation (%)	Wall thickness (mm)	Axial radius of curvature (r_z) (mm)	Circumferential radius of curvature (r_θ) (mm)
<i>Irradiated</i>							
O150-2	423	127	—	18	0.64	∞	4.93
O150-1L	423	127	5910	23	0.62	∞	5.16
O150-2L	423	130	6100	11	0.61	∞	4.66
O270-2	543	97	—	14	0.65	∞	4.76
O270-1L	543	93	4650	11	0.62	∞	4.63
O270-2L	543	94	4650	9	0.65	∞	4.57
O450-3	723	71	—	10	0.67	∞	-
O450-4	723	70	—	7	0.67	∞	-
O450-1L	723	66	3210	8	0.66	∞	4.50
O450-2L	723	66	3300	6	0.66	∞	4.44

All these data were obtained by measuring the parameters of each test during post-test examinations. Further research was aimed at determining correlation of burst pressure, circumferential elongation and true hoop stress at rupture versus temperature, type of cladding, and biaxiality ratio (see Fig. 2.7–Fig. 2.9, Table 2.7). In doing so, the true hoop stresses at rupture was calculated in compliance with the procedures previously developed for the high temperature burst tests and described in detail in [1].

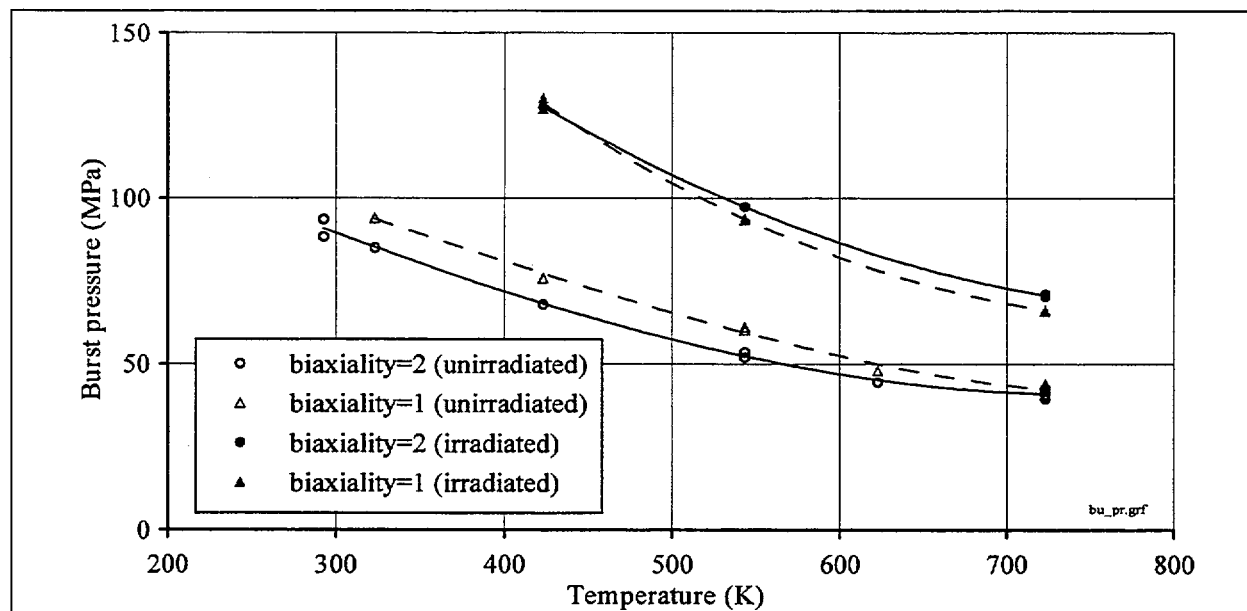


Fig. 2.7. Burst pressure versus temperature.

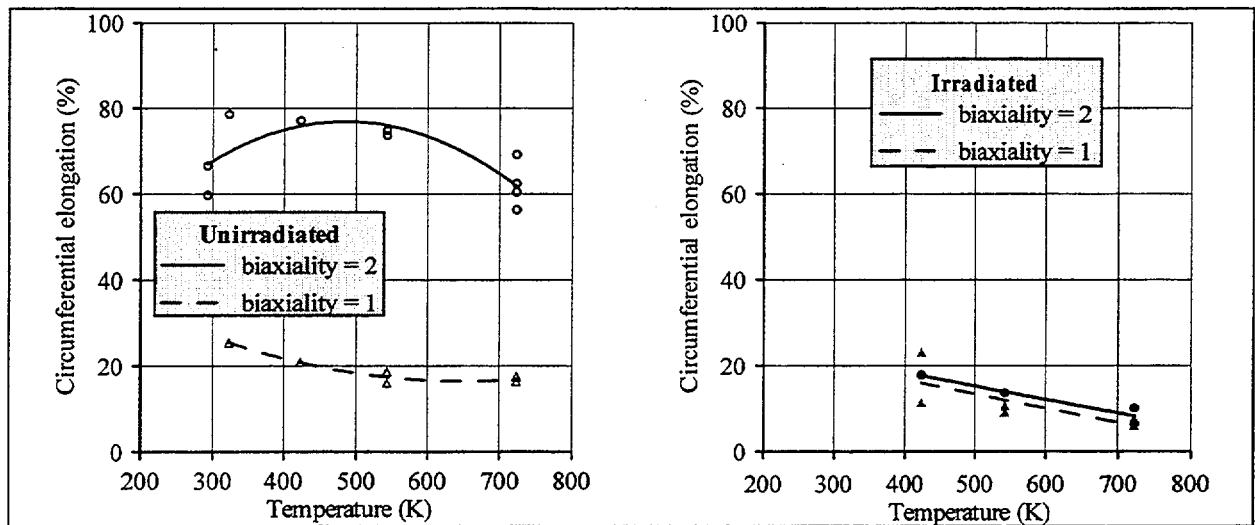


Fig. 2.8. Circumferential elongation versus temperature.

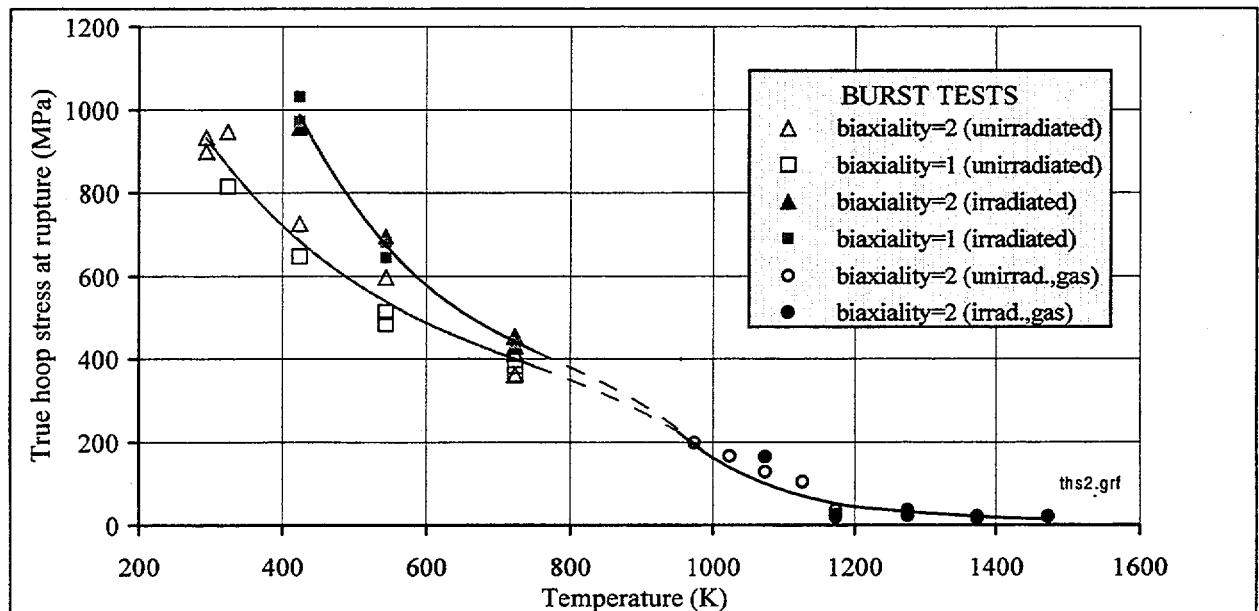


Fig. 2.9. True hoop stress at rupture versus temperature.

Table 2.7. Correlations for burst parameters versus temperature, biaxiality and type of cladding.

Parameter	Type of specimen	
	unirradiated	irradiated
Burst pressure (biaxiality=2)	$P_b = 151.8598267 - 0.2129816731 \cdot T - 2.886992355 \cdot 10^{-5} \cdot T^2 + 1.5397377 \cdot 10^{-7} \cdot T^3$	$P_b = 343.7481701 - 0.7161358707 \cdot T + 0.0004830832312 \cdot T^2$
Burst pressure (biaxiality=1)	$P_b = 135.3007207 - 0.06537602349 \cdot T - 0.0002851021788 \cdot T^2 + 2.7312947 \cdot 10^{-7} \cdot T^3$	$P_b = 400.4533641 - 0.9828090696 \cdot T + 0.00091965903 \cdot T^2 - 2.7630515 \cdot 10^{-7} \cdot T^3$
Circumferential elongation (biaxiality=2)	$\varepsilon_\theta = 13.97035999 + 0.2589695178 \cdot T - 0.0002665684037 \cdot T^2$	$\varepsilon_\theta = -0.0315744 \cdot T + 31.079106$

Parameter	Type of specimen	
	unirradiated	irradiated
Circumferential elongation (biaxiality=1)	$\varepsilon_{\theta} = 52.50524937 - 0.1112964864 \cdot T + 8.598062059 \cdot 10^{-5} \cdot T^2$	$\varepsilon_{\theta} = -0.0334367 \cdot T + 30.16835$
True hoop stress (biaxiality=1, 2)	$293 \leq T \leq 723$ $\sigma = 2016.268 - 5.2948 \cdot T + 0.00627 \cdot T^2 - 2.8233 \cdot 10^{-6} \cdot T^3$	$423 \leq T \leq 723$ $\sigma = 4178.356 - 12.894 \cdot T + 0.0154 \cdot T^2 - 6.5545 \cdot 10^{-6} \cdot T^3$
True hoop stress (biaxiality=2)	$973 \leq T \leq 1190$ $\sigma = \exp(-0.0065753 \cdot T) \cdot 116139.0182$ $1190 \leq T \leq 1473$ $\sigma = \exp(-0.004283 \cdot T) \cdot 7611.8232$	

Analysis of the array of these results showed the following:

1. Strength of irradiated cladding was significantly higher, than that of the unirradiated ones, with the burst pressure difference being approximately 40 MPa throughout the entire temperature range of the tests.
2. With the temperature increase, the burst pressure reduced monotonically, and was less dependent on biaxiality ratio.
3. True hoop stress at rupture for irradiated cladding was significantly higher than that of the unirradiated one, however, with the temperature increase this difference was reducing monotonically. We can consider with adequate reliability, that the true hoop stress at rupture for irradiated cladding is independent of the biaxiality ratio. As for the unirradiated cladding, the growth of the biaxiality ratio from 1 to 2 causes an increase of the hoop stress at rupture. However, significance of this effect reduces as the temperature rises, and the difference practically disappears at the temperature of 723 K. The general trend for the correlations obtained for irradiated and unirradiated specimens within the temperature range 293–723 K agrees with the data previously obtained for the high-temperature region (973–1473 K) [1]. This proves both the correctness of the experimental and analytical procedures used, and the absence of significant additional physical effects influencing the cladding behavior.
4. Circumferential elongation of unirradiated claddings is highly sensitive to the biaxiality ratio. When the biaxiality ratio increases, the cladding elongation sharply increases up to 60–75 %. Sensitivity of irradiated claddings to this ratio is very low. However, irradiated claddings showed dependence of hoop elongation versus temperature. Elongation was monotonically reduced with the increase of temperature.

3. CONDITION, PROCEDURES AND RESULTS OF AXIAL TENSILE TESTS

3.1. Test procedure and specimen design

Axial tensile tests with tube specimens are specified in Russia with a special standard [4]. Still accounting for the international character of this program it was decided to perform comparative reassessment for the standards used for these purposes in the Russian Federation, U.S. and France.

U.S. Standard ASTM E8M-93 [5].

According to this standard small diameter tubes ($D \leq 25$ mm) are usually tested as sections of a bulk cross-section tube. The main standard requirements to specimen and tooling, are shown on Fig. 3.1.

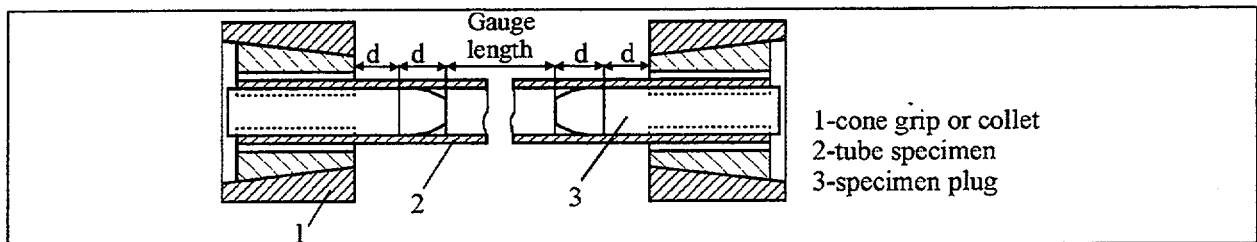


Fig. 3.1. Design of tube specimen according to the U.S. Standard.

Cone grips or collet grips are used for tests. Plugs should be used in both ends of the specimen. Two sizes are strictly stipulated:

- the spacing interval between the butt ends of the plugs equals the gauge length;
- the spacing interval between the machine jaws should be longer than the gauge length by four internal diameters of the specimen.

French Standard EN10002-5:1991 [6].

The specimen sizes according to the French standard are shown on Fig. 3.2. The main differences from the American standard are:

- the plugs used are of the cylindrical shape;
- the gauge length (l_g) is set smaller than the spacing interval between the butt ends of the plugs (L_c);
- the length of tube specimens (L_t) should be longer than the gauge length by two external diameters (D_o).

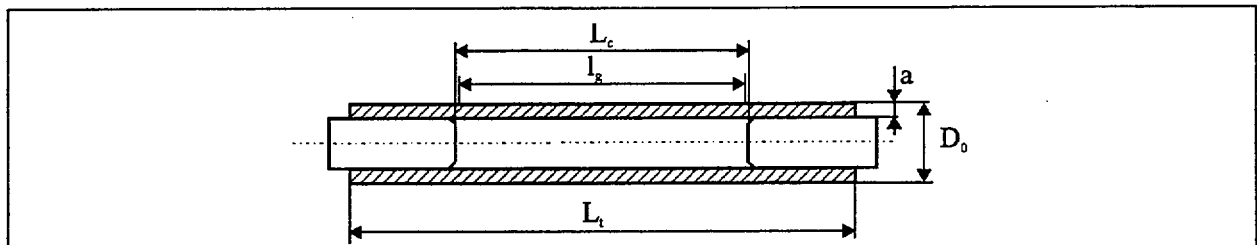


Fig. 3.2. Design of tube specimen according to the French Standard.

Russian Standard GOST 10006-80 [4].

The requirements of the Russian standard to the shape and sizes of tubular specimens are shown in Fig. 3.3.

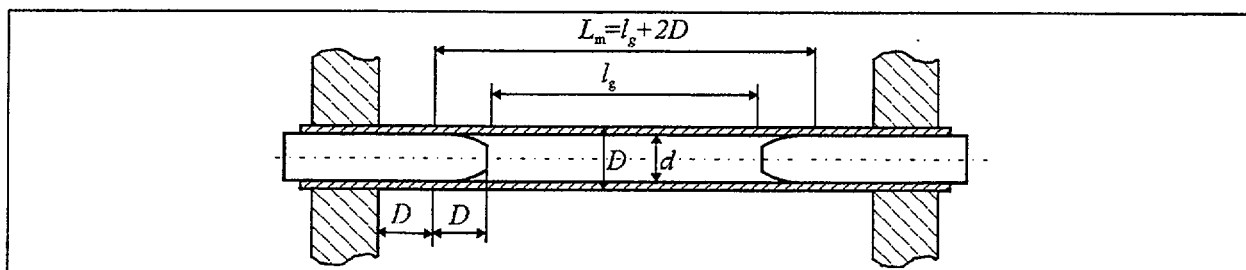


Fig. 3.3. Design of tube specimen according to the Russian Standard.

This standard integrates the requirements of both U.S. and French standards:

- the use of both conical and cylindrical plugs is enabled;
- every plug should go into a sample on a length not less than four diameters;
- the gauge length (l_g) is set smaller than the spacing interval between butt ends of the plugs (as in the French standard);
- the spacing interval between machine jaws should be longer than the gauge length by four diameters of the tubular specimens (as in the American standard), but the external ones (as in the French standard);
- a special marking is put on the specimen length (L_m) exceeding the gauge length by two external diameters (in the French standard it is the overall sample length) and allows afterwards to conduct the refinement of the elongation of a sample by matching the point of fracture with the middle of the gauge length.

Specimen design.

Analysis results of the of the reviewed standards requirements and features of the used testing machines were allowed for specimen design. The gauge length was set in accordance with the requirement of the Russian standard based on the following term:

$$l_g = 5.65 \sqrt{\frac{\pi}{4} (D^2 - d^2)}.$$

Two designed types of plug and specimen attachment are shown on Fig. 3.4. Plugs with special head for machine mandrels were used in case of unirradiated specimens (see Fig. 3.4a). In this case plugs and specimen were joined by means of welding. Such a design is a compromise with respect to all reviewed standards. In this case the deviation in the spacing interval between machine jaws has no value as the effort is transmitted by weld joint, instead of friction.

Collet grips were used for irradiated samples in the temperature range of 293–723 K. Such a design does not also greatly contradict the reviewed standards and allows one to eliminate the weld joint which would have lead to the annealing of the irradiated material and, as a result, to systematic errors in the measurements. Nevertheless, mechanical tests of irradiated specimens of temperatures above 1000 K were performed for the same specimen design as for the unirradiated cladding because annealing of irradiation damage in the whole of the specimen will most evidently take place under these high temperatures.

Special marks were put on all samples as hairlines of 30–40 μm depth and ~5 mm arc length in order to validate and to adjust the gauge length of the samples. These marks were put on along the length of 45 mm with a step of 1 mm. Besides, additional scoping tests were performed to certify test devices. Results of these tests have demonstrated that:

- ⇒ measurement uncertainty of the axial load was $\pm 1\%$;
- ⇒ measurement uncertainty of the test temperature was ± 3 K for the temperature range of 293–723 K, and ± 8 K for the temperature range of 1000–1200 K.

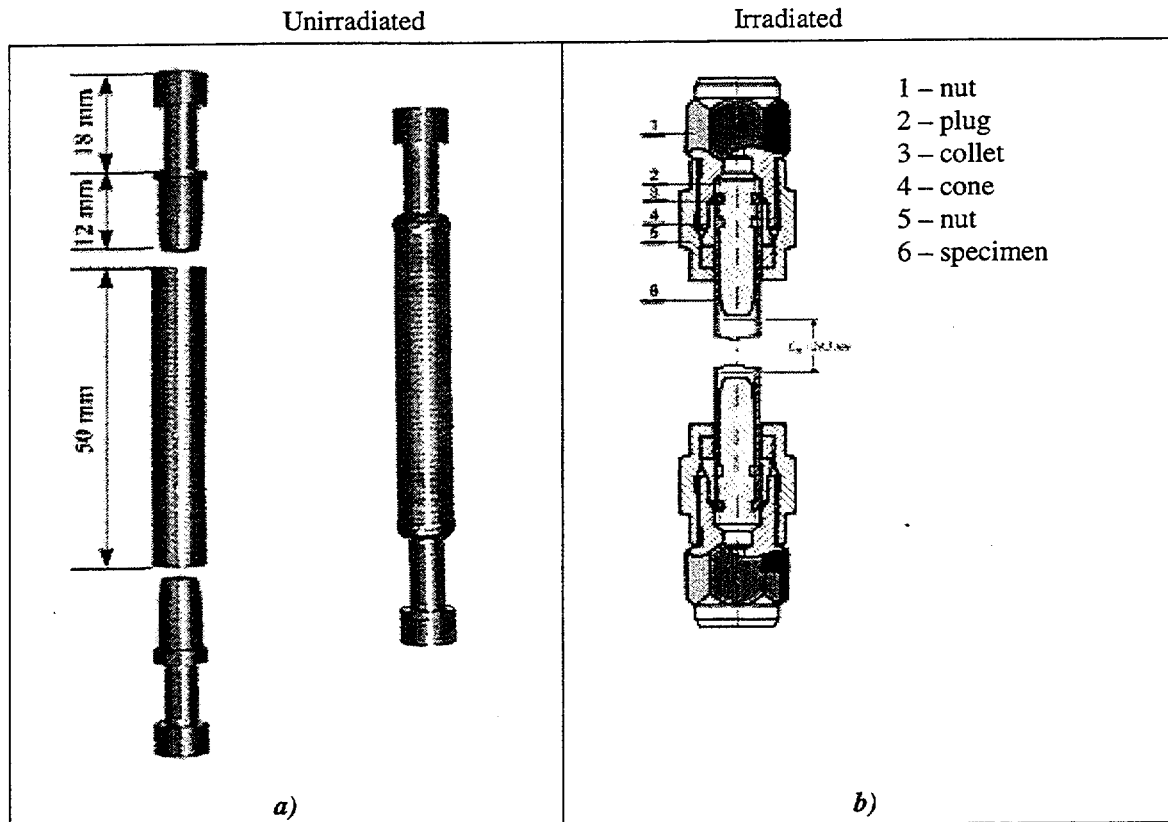


Fig. 3.4. Design of Zr-1%Nb tube specimen used for axial tensile tests.

Two test machines were used for the whole set of research. Low temperature tests were performed with the air inside the machine. Vacuum (up to 10^{-4} mm mercury) was used to reach high temperature test conditions (1000–1200 K).

Approach to adjust the specimen gauge length.

As was mentioned above, special attention was paid to the specimen gauge length while developing procedures for the axial tensile tests.

Special test was performed with irradiated specimen according to the following scenario:

- ⇒ load relief was arranged periodically during the loading test (see Fig. 3.5);
- ⇒ the first load relief was arranged close to the yield stress point;
- ⇒ the second one was arranged in the section between the yield stress and the ultimate strength;
- ⇒ the third relief was arranged close to the ultimate strength.

In addition to the major goal, this test was used to verify elastic properties of the mechanical system (including the specimen and machine). Data presented in Fig. 3.5 indicate that the apparent elastic modules of this system ($\text{tg}\alpha_1$) preserve high stability during the whole process of loading.

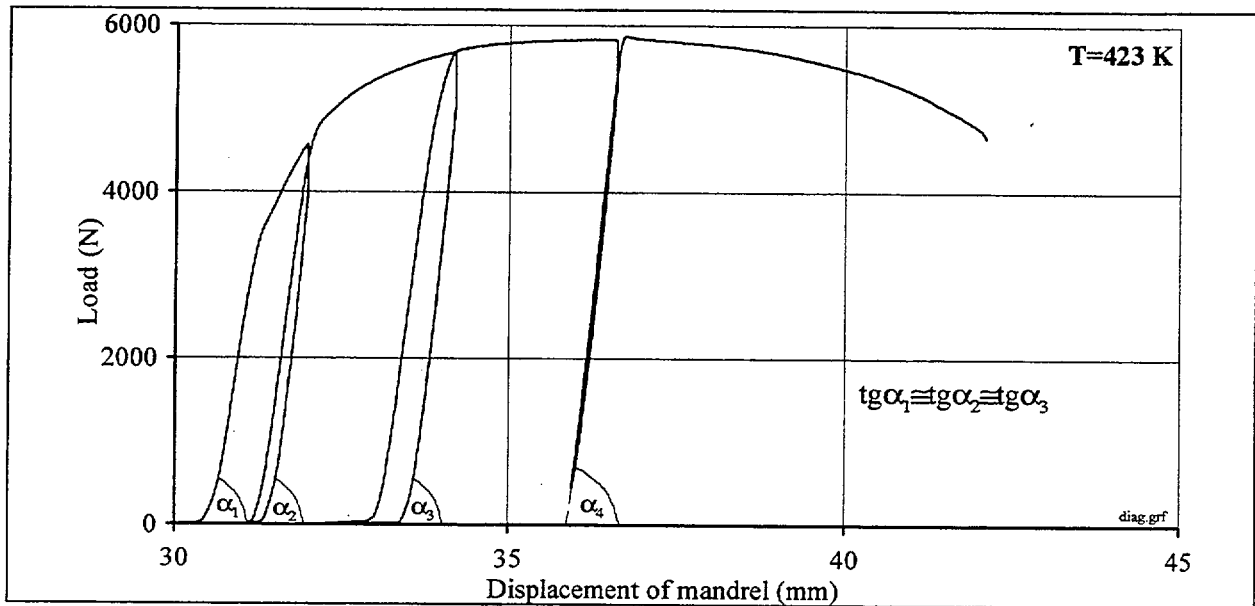


Fig. 3.5. Load-displacement curve.

This check has proved that the obtained load displacement curves, processed according to the standard procedures, allows one to determine the correct values of the specimen elongation.

An additional procedure was developed to use this test for validation of the specimen gauge length. This procedure included measurements of the intervals between special marks put onto the specimen (with a space of 1 mm) before the test. After that, the increment of the interval initial length was determined for three representative points of the load displacement curve:

- ⇒ yield stress area (after the first load relief);
- ⇒ intermediate area between the yield stress and the ultimate strength (after the second load relief);
- ⇒ rupture area (after the test).

Fig. 3.6 presents the results of these tests.

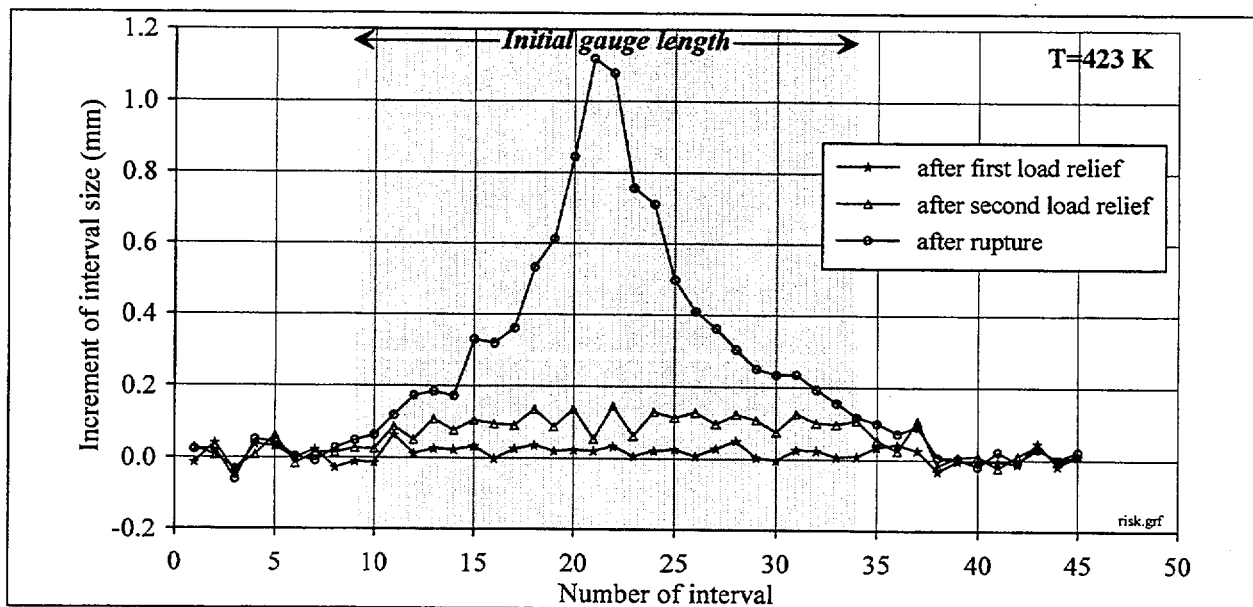


Fig. 3.6. Increment of interval between marks versus specimen length.





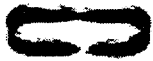

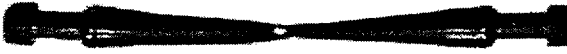


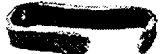
One could see that the deformation distribution along the sample length is of a symmetrical nature, the failure has taken place in the central part of a sample, and the main portion of deformation is concentrated within the bounds of the gauge length during the all test.

3.2. Results of axial tensile tests

Typical appearance of the specimen after uniaxial tests is represented in Table 3.1, Table 3.2.

Typical appearance of two types of the uniaxial tests is presented in the above tables to compare mechanical behavior of Zr-1%Nb cladding versus the load direction and temperature.

Table 3.1. Appearance of unirradiated specimens after tensile tests.

Temperature (K)	Tube specimen (axial tests)	Ring specimen (transverse tests)
293		
423		
543		 (623 K)
723		
1000		 (923 K)
1200		 (1223 K)

These results indicate that the earlier revealed (for ring specimens) tendency of sharp increase of the sample elongation is observed around 1000 K. With further temperature increase, the elongation noticeably decreases.

Processing of all stress-strain curves, measured in axial tests, allowed us to obtain the set of mechanical properties of Zr-1%Nb cladding presented in Table 3.2.

Table 3.2. Main results of axial tensile tests.

Number of test	T (K)	Yield stress (MPa)	Ultimate strength (MPa)	Total elongation (%)	Uniform elongation (%)
<i>Unirradiated</i>					
T20-2	293	237	378	45.1	18.5
T150-1	423	196	311	43.1	19.4
T270-5	543	118	225	54.1	28.3
T450-3	723	100	176	49.1	21.7
T450-7	723	99	184	54.1	20.2
T727-2	1000	56	59	-	7.9
T927-2	1200	8.6	11.6	80.6	5.7

Number of test	T (K)	Yield stress (MPa)	Ultimate strength (MPa)	Total elongation (%)	Uniform elongation (%)
<i>Irradiated</i>					
T50-0	323	520	585	18.3	2.8
T150-0-1	423	498	553	9.4	2.0
T150-0-2	423	516	572	13.0	3.1
T270-0-1	543	440	485	11.5	2.5
T270-0-2	543	409	461	14.2	2.0
T450-0-w	723	300	342	20.0	1.7
T450-0-2	723	317	326	12.9	1.2
T727-0-w	1000	51	52	-	3.3

The generalized data on uniaxial tensile tests in transverse and axial directions are presented in Fig. 3.7 – Fig. 3.10 in order to perform comparative analysis of all the uniaxial test results.

It should be noted, that these plots contain the results of recent additional ring tensile tests of irradiated specimens in temperature range of 673–773 K. The tests were performed in order to define more exactly the temperature dependencies of mechanical properties in transverse direction and to compare with axial test data. Ring specimens have been made from the irradiated claddings, which were used for axial tensile tests (see section 1.2 of this report). The results of additional ring tensile tests do not practically affect previously obtained temperature dependencies, so Fig. 3.7 – Fig. 3.10 contain the same correlations that were published in [1]. The new results of transverse tests are also presented in Table 3.3.

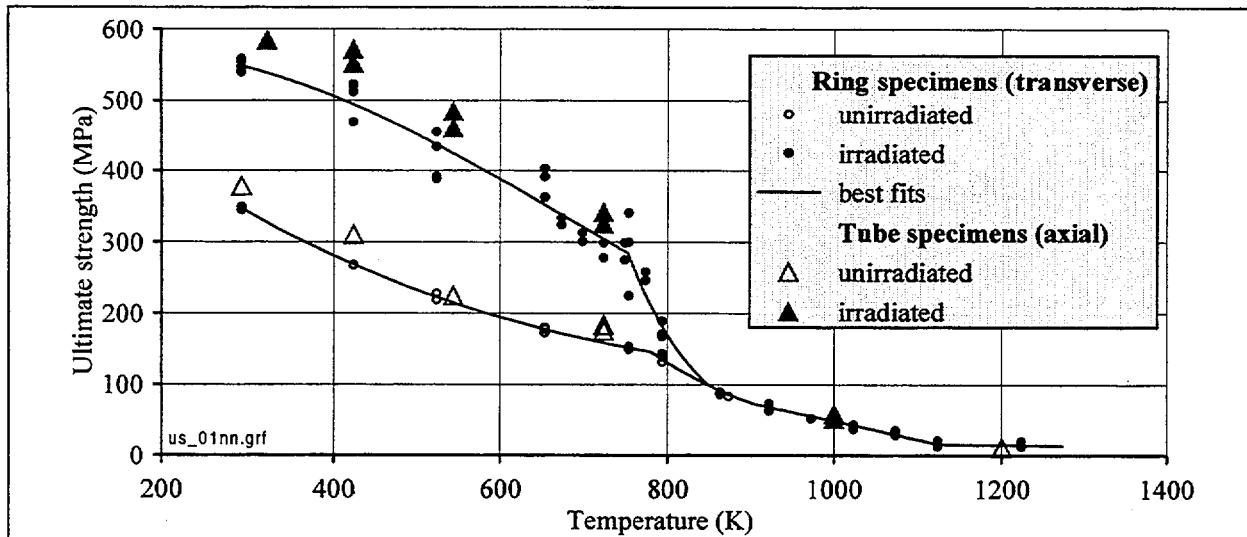


Fig. 3.7. Ultimate strength versus temperature.

Circles indicate the results of tests in the transverse direction; triangles indicate those in the axial direction. Light marks relate to unirradiated specimens, the black ones to irradiated specimens. The correlations presented were obtained from the results of tests in the transverse direction. The procedure for the obtainment of those is described in detail in [1].

The analysis of the ultimate strength data allows to reveal the following. At low temperatures, the ultimate strength in the axial direction is approximately 10% higher than that in the transverse direction. With temperature increase, this difference disappears. In the high temperature region, the values of the ultimate strength in the transverse and axial directions coincide. The noted tendency is equally valid both for unirradiated claddings and for the irradiated ones. Thus, the increase in the ultimate strength due to the irradiation in the reactor is similar in the transverse and axial directions.

Table 3.3. Results of simple ring tensile tests on irradiated Zr-1%Nb cladding (strain rate 0.002 1/s).

Temperature (K)	Ultimate strength (MPa)	Yield stress (MPa)	Total elongation (%)	Uniform elongation (%)
673	324	296	12.3	3.9
	334	319	13.0	2.7
698	313	293	11.0	2.4
	301	280	12.3	4.2
723	299	270	11.4	4.9
	278	258	10.5	4.0
748	299	278	10.8	3.4
	275	254	14.4	4.2
773	246	222	12.8	3.6
	258	240	18.4	3.5

The effect of the base irradiation on the yield stress in the transverse and axial directions manifests itself differently. In the low temperature range, the yield stress in the axial direction for unirradiated samples is approximately 30% less than that in the transverse direction, and for irradiated specimens, the yield stress in the axial direction is approximately 10% higher than that in the transverse direction. With temperature increase, this difference decreases as well as for the ultimate strength. Thus, the increase in the yield stress due to the reactor base irradiation is significantly higher in the axial direction than in the transverse one.

The observed loading direction effect on the yield stress and the ultimate strength for unirradiated samples is a consequence of Zr-1%Nb alloy anisotropy and quantitatively well matches the published data [7]. For irradiated samples, the effect of the loading direction essentially decreases indicating that the irradiation reduces the anisotropy of the yield stress for Zr-1%Nb alloy.

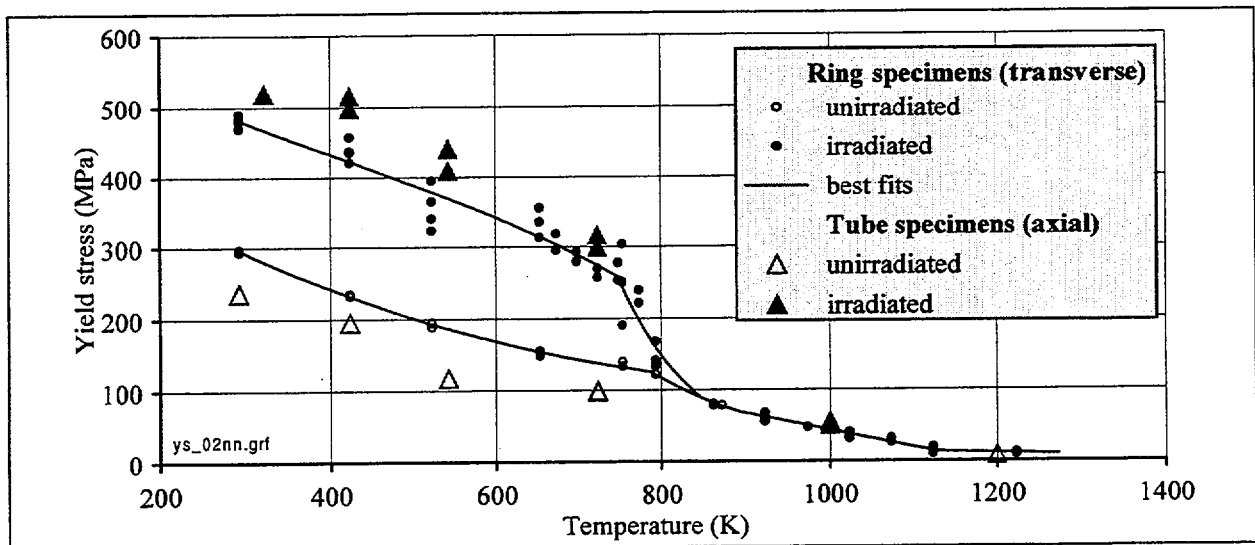


Fig. 3.8. Yield stress versus temperature.

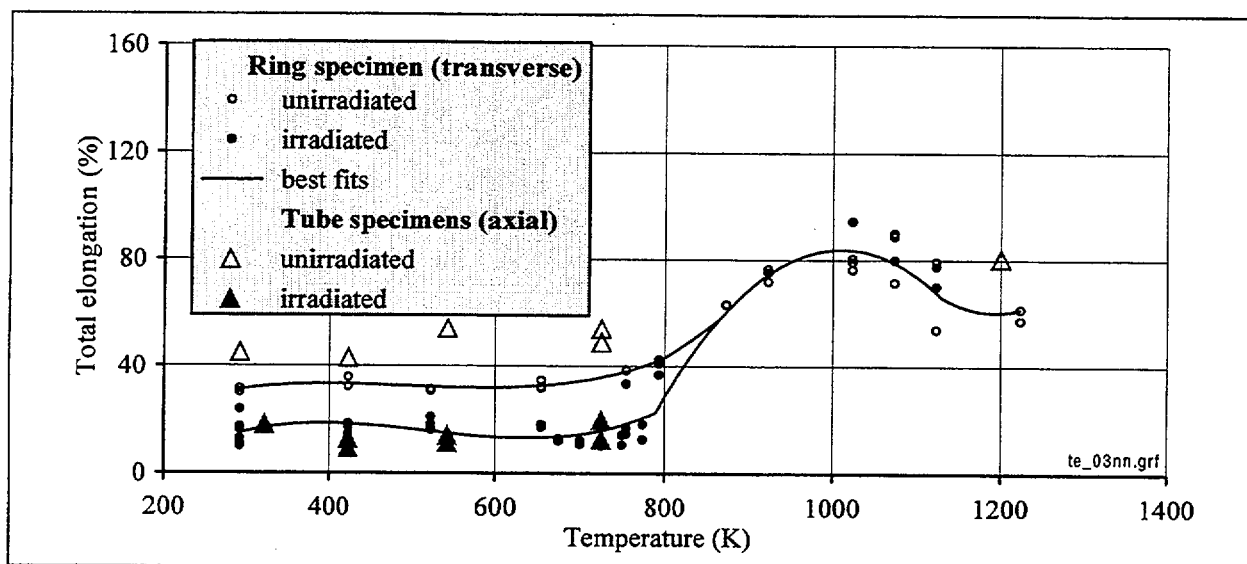


Fig. 3.9. Total elongation versus temperature.

Comparative analysis of the test data, characterizing total elongation of the cladding versus irradiation degree and temperature, leads to the following observations:

- ⇒ anisotropy of the unirradiated Zr-1%Nb cladding specimen takes place in the low temperature zone;
- ⇒ no pronounced anisotropy of irradiated cladding was registered in any of the temperature regions.
- ⇒ total elongation versus temperature for both specimen types and in both directions can be divided into three typical zones, the boundaries of which correspond to the temperatures of allotropic phase transformations of Zr-1%Nb alloy (see Fig. 3.9):
 - total elongation of the α phase of Zr-1%Nb alloy slightly depends on the temperature;
 - abrupt increase of the total elongation takes place during $\alpha + \beta$ phase of Zr-1%Nb alloy;
 - total elongation gets significantly less when transferring to the β phase of Zr-1%Nb alloy.

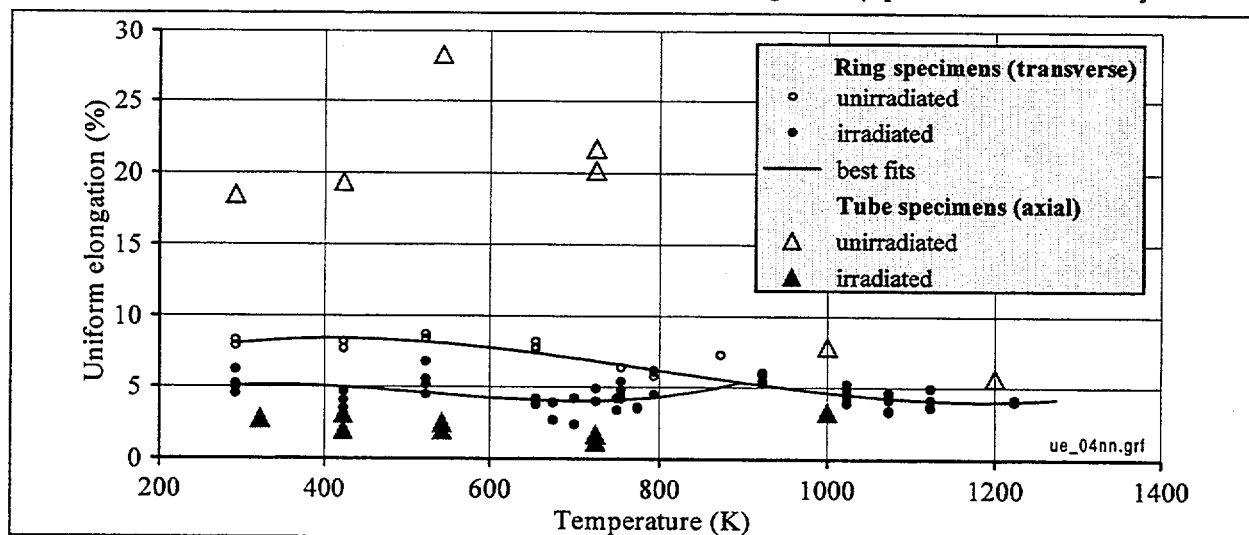


Fig. 3.10. Uniform elongation versus temperature ($\dot{\epsilon}=2 \cdot 10^{-3} \text{ s}^{-1}$).

The analysis of the uniform elongation data shows that this parameter depends strongly on the loading direction. For unirradiated samples, the uniform elongation in the axial direction under low temperatures significantly (several times) exceeds that in the transverse direction. For irradiated samples, the uniform elongation in the axial direction is moderately less than that in the transverse direction. As the temperature in-

creases, the influence of the irradiation and loading direction over the uniform elongation diminishes as in the case for the ultimate strength, the yield stress and the total elongation.

The revealed sharp decrease of the uniform elongation in the axial direction due to the irradiation is the important result. A careful analysis of the experimental procedures showed up the lack of significant systematic errors in measurements.

It should be also noted that a sharp decrease of the uniform elongation in the axial direction due to the irradiation is qualitatively in accord with the results of measurements of ultimate strength (US) and yield stress (YS). Fig. 3.11 illustrates US/YS ratio versus the temperature for the irradiated and unirradiated samples tested in the transverse and axial directions. The US/YS ratio characterizes the material potentiality for the strain hardening and, consequently, must correlate with the uniform elongation value. As can be seen from Fig. 3.11, the US/YS ratio for unirradiated samples tested in the axial direction under the temperatures lower than 800 K is significantly higher than that for the other specimens.

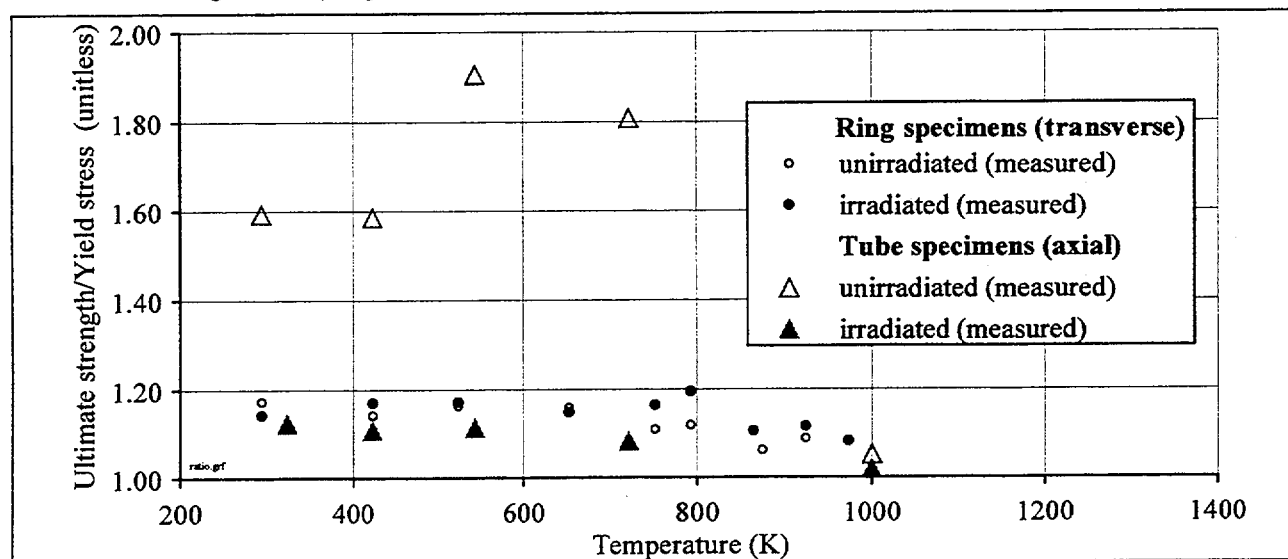


Fig. 3.11. US/YE ratio versus temperature.

The obtained results indicate an essential change in the anisotropy of Zr-1%Nb alloy mechanical properties at high burnup. In the course of a base irradiation, the cladding is not only subjected to radiation damages but also accumulates residual strains caused by the coolant excessive pressure and PCMI during power ramps. The total influence of those factors leads to different changes of mechanical properties in the axial and transverse directions.

Results of the axial tensile tests presented in this section, as well as the results of the comparative analysis of both types of uniaxial tensile tests allow us to consider that this database together with the database obtained due to biaxial burst tests can be the basis to determine anisotropy coefficients, deformation law, and to develop failure criteria for Zr-1%Nb cladding.

4. CONCLUSIONS

New research was performed to study mechanical properties of unirradiated and irradiated Zr-1%Nb cladding. The objective of the previous program was to measure mechanical properties of Zr-1%Nb cladding in the transverse direction, and under the high temperature internal gas loading conditions (burst tests). The present program was designed to determine mechanical properties in the axial direction, and to obtain mechanical properties of Zr-1%Nb cladding for low temperature biaxial loading (burst tests).

Results of these tests lead to the following conclusions:

1. Axial tensile tests showed the same general tendencies of the cladding mechanical properties obtained with uniaxial tests in the transverse direction. These are: irradiation of Zr-1%Nb cladding leads to the increase of the cladding strength and to the decrease of the cladding ductility in the low temperature range. The difference between mechanical properties of unirradiated and irradiated claddings disappears completely at the temperatures above 860 K.
2. Low temperature burst tests have demonstrated high sensitivity of the circumferential elongation of unirradiated claddings to biaxiality ratio. Strength parameters of both types of claddings and circumferential elongation of irradiated cladding are independent of the biaxiality ratio.
3. Analysis of all the summarized mechanical data shows that the anisotropy effect is insignificant for irradiated cladding in the whole temperature range studied. Anisotropy effect is very evident in unirradiated claddings for the yield stress, uniform elongation, and total elongation at low temperatures.
4. Results of the axial tensile tests and low temperature biaxial burst tests along with the results of the previously performed transverse tensile tests, and high temperature burst tests will be used as the basis to determine the anisotropy coefficients of Zr-1%Nb cladding versus temperature, as well as to develop the deformation laws for thermal mechanical codes. In addition to that, the test results could be used to develop the cladding failure criteria under low and high temperature conditions.

References

- [1] L.Yegorova, V.Asmolov, G.Abyshov, V.Malofeev, A.Avvakumov, E.Kaplar, K.Lioutov, A.Shestopalov, A.Bortash, L.Maierov, K.Mikitiouk, V.Polvanov, V.Smirnov, A.Goryachev, V.Prokhorov, and A.Vurim "Data Base on the Behavior of High Burnup Fuel Rods with Zr-1%Nb Cladding and UO₂ Fuel (VVER Type) under Reactivity Accident Conditions", RRC "Kurchatov Institute" report NSI RRC 2179, Vol.2, 1999 (also USNRC report NUREG/IA-0156 and IPSN report IPSN 99/08 - 2).
- [2] A.Shestopalov, K.Lioutov, L.Yegorova, G.Abyshov, K.Mikitiouk "Modification of U.S. NRC's FRAP-T6 Fuel Rod Transient Code for High Burnup VVER Fuel", RRC "Kurchatov Institute" report NSI RRC 2180, 1999 (also USNRC report NUREG/IA-0164 and IPSN report IPSN 99/10).
- [3] K.Mikitiouk, A.Shestopalov, K.Lioutov, L.Yegorova, G.Abyshov "Modification of IPSN's SCANAIR Fuel Rod Transient Code for High Burnup VVER Fuel", RRC "Kurchatov Institute" report NSI RRC 2181, 1999 (also USNRC report NUREG/IA-0165 and IPSN report IPSN 99/09).
- [4] GOST 10006-80 Metallic tubes – Procedure of tensile tests (rus.)
- [5] ASTM E8M-93 Standard Test Methods for Tension of Metallic Materials (Metric).
- [6] EN10002-5:1991 Materials metalliques- Essai de traction-Partie 5: Methode d'essai a temperature elevee.
- [7] A.Zaimovskyi, A.Nikulina, N.Reshetnikov "Zirconium Alloys in the Nuclear Industry". Moscow, Energoizdat, 1981 (rus).

BIBLIOGRAPHIC DATA SHEET

(See instructions on the reverse)

1. REPORT NUMBER
(Assigned by NRC, Add Vol., Supp., Rev.,
and Addendum Numbers, if any.)

NUREG/IA-0199
IPSN 01-16
NSI RRC 2241

2. TITLE AND SUBTITLE

Mechanical Properties of Unirradiated and Irradiated Zr-1%Nb Cladding
Procedures and Results of Low Temperature Biaxial Burst Tests and Axial
Tensile Tests

3. DATE REPORT PUBLISHED

MONTH	YEAR
April	2001

4. FIN OR GRANT NUMBER

5. AUTHOR(S)

E. Kaplar, L. Yegorova, K. Lioutov, A. Konobeyev, N. Jouravkova, NSIRRC
V. Smirnov, A. Goryachev, V. Prokhorov, O. Makarov, S. Yerebin, A. Svyatkin, RIAR

6. TYPE OF REPORT

Technical

7. PERIOD COVERED (Inclusive Dates)

8. PERFORMING ORGANIZATION - NAME AND ADDRESS (If NRC, provide Division, Office or Region, U.S. Nuclear Regulatory Commission, and mailing address; if contractor, provide name and mailing address.)

Nuclear Safety Institute of Russian Research Centre "Kurchatov Institute" Kurchatov Square 1, Moscow 123182 Russian Federation

State Research Centre "Research Institute of Atomic Reactors" Dimitrovgrad 433510, Russian Federation

9. SPONSORING ORGANIZATION - NAME AND ADDRESS (If NRC, type "Same as above"; if contractor, provide NRC Division, Office or Region, U.S. Nuclear Regulatory Commission, and mailing address.)

Division of Systems Analysis and Regulatory Effectiveness
Office of Nuclear Regulatory Research
U.S. Nuclear Regulatory Commission
Washington, DC 20555-0001

10. SUPPLEMENTARY NOTES

11. ABSTRACT (200 words or less)

The present program was designed to determine mechanical properties in the axial direction, and to obtain mechanical properties of Zr-1%Nb cladding for low temperature biaxial loading (burst tests).
Results of these tests lead to the following conclusions:

1. Axial tensile tests showed the same general tendencies of the cladding mechanical properties obtained with uniaxial tests in the transverse direction. These are: irradiation of Zr-1%Nb cladding leads to the increase of the cladding strength and to the decrease of the cladding ductility in the low temperature range. The difference between mechanical properties of unirradiated and irradiated claddings disappears completely at the temperatures above 860 K.
2. Low temperature burst tests have demonstrated high sensitivity of the circumferential elongation of unirradiated claddings to biaxiality ratio. Strength parameters of both types of claddings and circumferential elongation of irradiated cladding are independent of the biaxiality ratio.
3. Analysis of all the summarized mechanical data shows that the anisotropy effect is insignificant for irradiated cladding in the whole temperature range studies. Anisotropy effect is very evident in unirradiated claddings for the yield stress, uniform elongation, and total elongation at low temperatures.

12. KEY WORDS/DESCRIPTORS (List words or phrases that will assist researchers in locating the report.)

Zirconium-1% Niobium alloy
burst tests
material properties
cladding strain and ballooning
test procedures
post-test examinations

13. AVAILABILITY STATEMENT

unlimited

14. SECURITY CLASSIFICATION

(This Page)

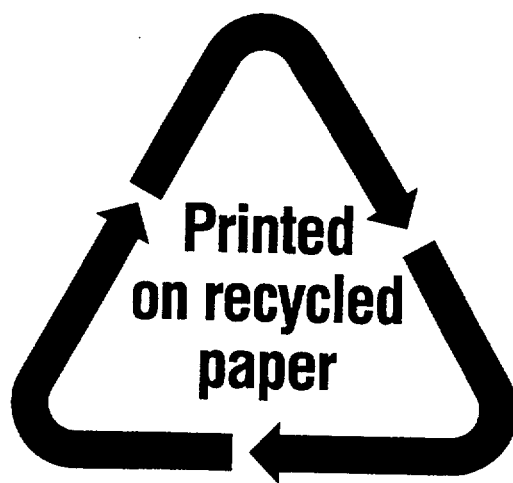
unclassified

(This Report)

unclassified

15. NUMBER OF PAGES

16. PRICE



Federal Recycling Program

UNITED STATES
NUCLEAR REGULATORY COMMISSION
WASHINGTON, DC 20555-0001

OFFICIAL BUSINESS
PENALTY FOR PRIVATE USE, \$300